Adsorption (2008) 14: 275–281
DOI 10.1007/s10450-007-9092-7

Hydrothermal stability of pelletized zeolite 13X for energy storage applications

G. Storch · G. Reichenauer · F. Scheffler · A. Hauer

Received: 30 April 2007 / Revised: 31 August 2007 / Accepted: 19 December 2007 / Published online: 18 January 2008

Abstract Three samples of pelletized zeolite Na-13X from different industrial suppliers were hydrothermally treated in an open system for up to 3500 adsorption/desorption cycles. Before and after this aging procedure, the samples have been characterized by water uptake measurements, X-ray powder diffraction (XRD), Hg-porosimetry, N_2- and CO_2-adsorption and small-angle X-ray scattering (SAXS). Large differences in the degree of degradation were found between the different materials: The adsorbent with the best performance maintains 79% of its original water uptake capacity after 3500 cycles, whereas this value is reduced to 65% after only 1600 cycles in case of the most unstable sample. For all materials, the residual water adsorption capacity was found to be higher than it was to expect from XRD data. In addition to structural changes of the zeolite cages, Hg-porosimetry and SAXS reveal a modification of the sample morphology in the meso- and macropore range. CO_2 adsorption experiments evidence that as a result of the aging process mass transfer kinetics are slowed down significantly.

These findings indicate that the influence of hydrothermal treatment on the water adsorption performance not only depends on the crystal structure of the actual adsorbent, but is indeed a result of a complex interplay with the system of larger pores. The crucial role of the binder material is underlined by the fact that the most stable sample was produced by a so-called binder-free method.

Keywords Gas phase adsorption · Adsorbents · Energy applications

G. Storch (✉) · A. Hauer
Division Technology for Energy Systems and Renewable Energy, Bavarian Center for Applied Energy Research (ZAE Bayern), Garching, Germany
e-mail: storch@muc.zae-bayern.de

G. Reichenauer
Division Functional Materials for Energy Technology, Bavarian Center for Applied Energy Research (ZAE Bayern), Würzburg, Germany

F. Scheffler
Division Thermal Sensing and Photovoltaics, Bavarian Center for Applied Energy Research (ZAE Bayern), Erlangen, Germany

1 Introduction

In recent years it has become clear that the only way to avoid irreversible changes to the world's climate and dramatic consequences of global warming is to cut down the level of carbon dioxide emissions. This can be achieved by making energy systems more efficient and by enhanced use of CO_2-neutral energy sources.

In this struggle, energy storage technologies play a key role when it comes to match energy availability, e.g. from regenerative energy sources or industrial waste heat, and peak demand periods.

Energy storage systems based on adsorption processes are promising candidates in this context, making use of the high heat of adsorption of water: For charging the storage, an adsorbent needs to be dehydrated by means of an available heat source. The dry adsorbent can be stored over very long periods. Discharging occurs by readsorption of water vapour, releasing the heat of adsorption.

First ideas for this kind of energy storage date to the 1970ies (Close and Dunkle 1977), originally aiming at a method for seasonal storage of solar energy. Currently several groups are working on the development and demonstration of adsorption energy storage, following the routes of evacuated (Stach et al. 2005; Jänchen et al. 2004; Gartler et

al. 2004; Nuñez et al. 2003; Mugele 2004) and open systems (Hauer 2002a, 2002b).

The energy storage density of adsorbents in closed cycle heat storage applications can be calculated via

$$\rho_Q = \int_{x_{S,des}}^{x_{S,ads}} \Delta h_{ads} dx_S \approx \overline{h_{ads}}(x_{S,ads} - x_{S,des}). \quad (1)$$

Hence, materials with high water uptake and binding energy are necessary. Hydrophilic zeolites, e.g. types LTA and especially 13X, show these properties in combination with a high temperature lift and are therefore very well suited for this kind of applications (Hauer 2002a, 2002b; Stach et al. 2005). However, these aluminium-rich adsorbents suffer from decomposition under hydrothermal conditions due to the attack of protons to the Al–O–Si bonds (Lutz et al. 2005; Buhl et al. 2004 and references therein):

$$H^+ + OH^- + Na^+ \equiv Al^- – O – Si \equiv$$
$$\leftrightarrow OH^- + Na^+ + \equiv Al + HO – Si \equiv$$

In energy storage applications, potentially detrimental conditions of high water vapour partial pressure in combination with elevated temperatures may arise frequently, especially during the desorption step.

Several studies have been carried out on the hydrothermal stability of zeolite LTA and FAU (Wolf et al. 1967; Lutz et al. 1983, 1988, 2005; Richtermendau et al. 1988; Fichtner-Schmittler et al. 1992; Ehrhardt et al. 1995; Buhl et al. 2004; Dimitrijevic et al. 2006). In these publications, a relation between the susceptibility of zeolites to hydrothermal damage and the Si/Al-ratio, as well as the dependency on the cation size in ion-exchanged zeolites was established (Buhl et al. 2004; Fichtner-Schmittler et al. 1992). However, with the exception of Lutz et al. (1988), powder samples were used in these previous experiments, and in the majority of cases, hydrothermal aging was performed in an autoclave under saturated steam conditions (except Wolf et al. 1967). Hence, quantitative transferability of these results to the case of open adsorption systems for heat storage is still uncertain. In these applications, adsorbent pellets containing inorganic binders are used. The most critical situation during the charging/discharging cycle arises when the gas stream used for desorption (T_{in} = 300–400 °C, $T_{d,in}$ up to 60 °C) is imposed on the fully adsorbed zeolite bed.

In the present study, industrial grade samples from different suppliers have been submitted to repeated adsorption/desorption cycles under conditions that are also expected in an application. Treated and untreated samples have been characterized extensively in order to shed light upon the degree of hydrothermal damage as well as on the microscopic nature of the decomposition process and the possible role of the binder material.

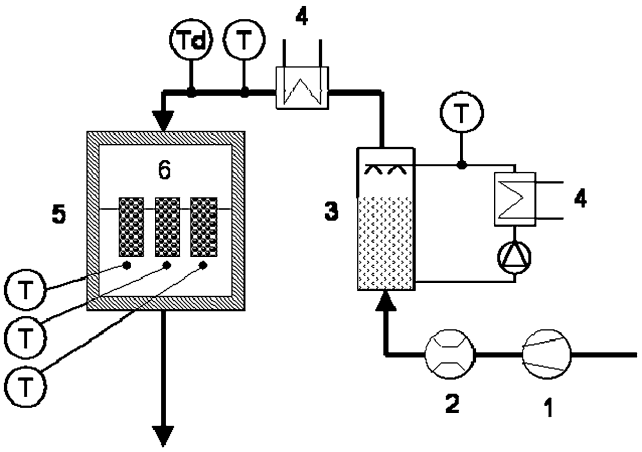

Fig. 1 Setup for adsorption/desorption cycling. (*1*) blower, (*2*) flow meter, (*3*) packed column humidifier, (*4*) heater, (*5*) insulation, (*6*) test columns. (*T*) temperature sensors, (*Td*) humidity sensors

2 Experimental

For this study, we have compared three different zeolite materials of identical type (zeolite 13X). All samples are pelletized standard material from industrial production lines of three different manufacturers (Table 1). Bead sizes vary from 1.5 to 5 mm. Materials 1 and 2 were conventionally produced using mainly clay minerals as a binder for pellet forming. Sample 3 originates from a so-called "binderless process" where actually LTA-type zeolite serves as a binder. Due to information protection, no further details about the binder materials used are available from the suppliers.

One sample of each material (1b, 2b, 3b) was subjected to hydrothermal aging by automated adsorption/desorption cycling in an open system (Fig. 1). The materials to be tested were contained as fixed beds in small test columns, measuring 0.15 m in height and 0.05 m in diameter, thus providing about 180 g of each material for the subsequent characterization experiments. The gas temperature at the outlet of the test columns was monitored individually for each sample. Air inlet conditions were T_{in} = 350 °C, $T_{d,in}$ = 50 °C for desorption and $T_{in} \approx T_{d,in}$ = 25 °C during adsorption at a superficial velocity of the gas flow of 0.5 m/s. Due to fluctuations in ambient air pressure, the water content x_G of the air at the column inlet varied between 0.09 and 0.1 kg/kg. Mode switching after adsorption and desorption occurred on all test columns attaining temperature thresholds of 60 °C and 200 °C, respectively, mimicking realistic application conditions. Thus, breakthrough of the mass transfer zone was complete but adsorption equilibrium was not attained throughout the whole test column during the cycling process. Together with a waiting time of 50 min to allow for cooling down of the test columns, 130 min were needed for the completion of an individual adsorption/desorption cycle.

Table 1 List of samples investigated

Sample	Trade name	Provenience	Treatment	Binder
1a	Köstrolith 13XK	CWK Bad Köstritz	As prepared	Clay mineral
1b	Köstrolith 13XK	CWK Bad Köstritz	1600 cycles	
2a	Sylobead MS C542	Grace Davison	As prepared	
2b	Sylobead MS C542	Grace Davison	3500 cycles	
3a	WEG 894	UOP	As prepared	Zeolite LTA
3b	WEG 894	UOP	3500 cycles	

Sample 1b was withdrawn from cycling after completion of 1600 cycles, showing already severe damage. In the case of samples 2b and 3b, hydrothermal aging was allowed to proceed over 3500 cycles.

After the hydrothermal treatment, the cycled samples as well as the as-prepared samples 1a, 2a, 3a were extensively characterized.

Dry weight and water adsorption were also determined by baking the samples in a laboratory furnace at 290 °C for 20 h and adsorption in an exsiccator at relative humidity $\varphi = 0.55$ during 70 h. The crystalline structure of all samples was characterized by X-ray diffraction on a *X'pert Pro* (*PANalytical*) under ambient conditions.

The specific surface area and micropore volume were determined by N_2-adsorption at 77 K with an ASAP 2000 (software ASAP 2010) volumetric sorption unit by Micromeritics. The samples were pretreated for degassing at 200 °C for >12 h in vacuum. Instrumental parameter equilibration interval was set to 35 s, resulting in typical total runtimes for a complete isotherm of about 20 h. The specific surface area was calculated by the BET-method (7-point) in the pressure range $p/p_0 = 0.03$–0.12 and the micropore volume was calculated using the t-plot method from statistical thickness values between 6 and 10 Å.

Complementarily, we measured CO_2-adsorption at 273 K on the same instrument. Prior to the adsorption measurement the sample was degassed under vacuum for several hours at 350 °C. For the adsorption run the parameter "equilibration interval" was set to 120 s. Typical equilibration times were about 6 hours for the first point of the isotherm taken and 1 to 2 hours for each subsequent dosing step. In order to verify whether equilibrium conditions were reached, a reference measurement with a manually prolonged waiting time of 3500 s was also performed. From these data, the limiting micropore volume was determined from a Dubinin-Radushkevich evaluation of the volume adsorbed in the relative pressure range $3{\cdot}10^{-5}$ to $5{\cdot}10^{-4}$.

Meso- and macropore volume was determined by Hg-porosimetry using Porosimeter 2000 (Carlo Erba) in the diameter range between 7.5 and 150 000 nm.

Small angle X-ray scattering (SAXS) is a versatile tool for investigating microporous structures, special benefits of this technique being its applicability to crystalline as well as to amorphous materials, and the independence of the porosity detected from the probe molecule and associated kinetic effects. Therefore, SAXS provides information on all meso- and micropores present as well as on non-porous density fluctuations, whereas sorption analysis only detects porosity accessible to the probing molecules. SAXS experiments were performed at the JUSIFA beamline of the HASYLAB synchrotron facility in Hamburg, Germany (Haubold et al. 1989). To cover a range in scattering vector from 0.2 to 8 nm^{-1}, two different sample-detector distances of 936 mm and 3600 mm were used. The energy of the incident X-ray was adjusted to about 12 keV. Scattering patterns were recorded using a two-dimensional position sensitive detector. One pellet of each sample was ground to a disc with parallel plane surfaces, its thickness being between 0.3 and 0.6 mm. During the experiment, the samples were kept under vacuum conditions. The measured scattering intensity was normalized to the sample thickness.

Table 2 Water sorption capacity x_S before and after hydrothermal aging. Note that the number of cycles in case of sample 1 b is less than half of the cycles applied to sample 2 b

Sample	x_S $\varphi = 0.55$	
	kg/kg	Relative
1a	0.23	100%
1b	0.15	65%
2a	0.24	100%
2b	0.14	59%
3a	0.26	100%
3b	0.20	79%

3 Results and discussion

After hydrothermal treatment, all samples show significant reduction of water uptake (Table 2). However, the extent of this effect varies considerably among the materials investigated, although all three of them are based on the same structural type of zeolite. Sample 3 proves to be the most stable under hydrothermal conditions, while sample 1 shows the

same damage as sample 2 already after only half the number of adsorption/desorption cycles.

The X-ray diffraction measurements (Fig. 2) show clearly the partial destruction of crystal structure during the cycling process. Diffraction peaks at values 7.25°, 12.55°, 16.21°, 21.71°, 24.01° and 27.21° for the angle 2θ in addition to the fingerprint of 13X correspond to the Miller-indices 200, 222, 420, 600/442, 622 and 642 of LTA-type zeolite and evidence its presence as a binder within samples 3 a/b. In previous experiments on powder samples, the reduction of water sorption capacity is explained by loss of crystallinity and was found to correlate well with decreasing X-ray peak intensity (Lutz et al. 2005). Table 3 shows the results of a quantitative analysis of the diffraction intensity after the aging process in relation to the value for the as-prepared samples. While the general trend of decreasing activity is well reproduced by these values, there is no direct quantitative correlation between X-ray crystallinity and water adsorption capacity (see also Fig. 4).

The same holds for microporosity as characterized with CO_2 and N_2 adsorption (Table 3): Experiments with both probe gases show a significant reduction in micropore volume and active adsorption surface. However, a quantitative agreement between these values as well as with the XRD and water uptake measurements is not given within the experimental error of the data (Fig. 4). This can in part be explained by the shortcomings of the BET model for describing adsorption phenomena on zeolites with their complex system of micro- and mesopores (Keller and Staudt 2005), the resulting value strongly depending on the pressure range and number of points used for fitting. Nevertheless, the BET method is being frequently used for the characterization of zeolitic adsorbents in a technical context and may be useful for the sake of relative comparison of samples, as in our case, if subjected to exactly the same data treatment.

Comparing the isotherms directly (Fig. 3), it can be seen that the slope in the range of $0.2 < p/p_0 < 0.8$ is more pronounced in case of the conventionally produced samples 1 (not shown) and 2. Together with the stronger capillary condensation at $p/p_0 > 0.9$, this indicates significantly more mesopores within these systems than in sample 3.

Due to the complex interplay between the active zeolite sites and the mesopore system inside the pellet created by means of the binder material, not only a change to the crystal structure may occur during hydrothermal treatment, but

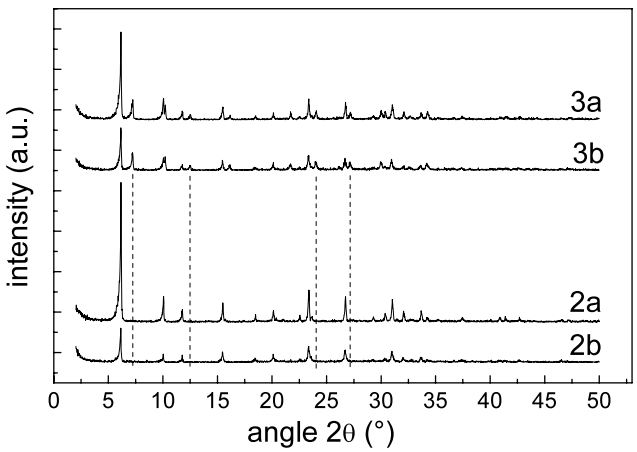

Fig. 2 XRD data of samples 2 a/b and 3 a/b. Note the additional peaks in the case of samples 3 a/b, indicated by the *dashed lines*

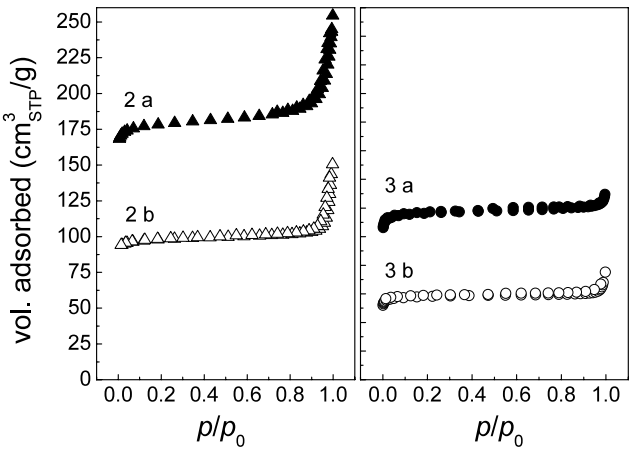

Fig. 3 Nitrogen adsorption isotherms for samples 2 and 3 before and after hydrothermal treatment. Note the steeper slope and enhanced capillary condensation in the case of sample 2, indicating higher porosity in the mesopore range

Table 3 Results from structural sample characterization. Bear in mind that BET surface for microporous samples is only an empirical benchmark for relative comparison

Sample	XRD-intensity (relative)	a_S BET (N_2) (m^2/g)	v_S (N_2) (cm^3/g)	v_S (CO_2) (cm^3/g)	v_S (Hg) (cm^3/g)
1a	100%	625	0.25	0.32	0.30
1b	56%	320	0.13	0.14	0.36
2a	100%	666	0.27	0.32	0.29
2b	50%	366	0.15	0.15	0.38
3a	100%	446	0.18	0.31	0.22
3b	73%	217	0.09	0.21	0.25

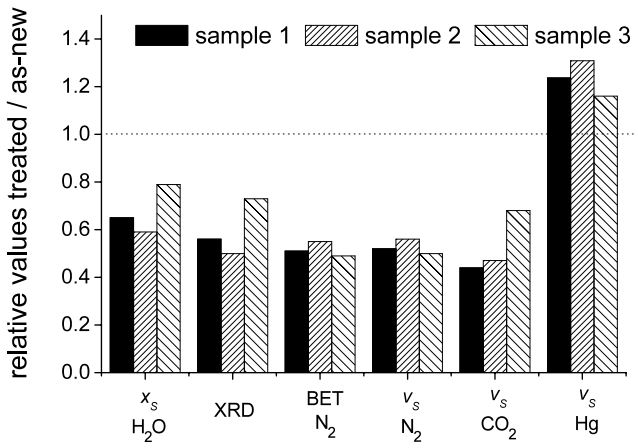

Fig. 4 Hydrothermal damage as evidenced by the different techniques (relative values, aged vs. as-prepared material)

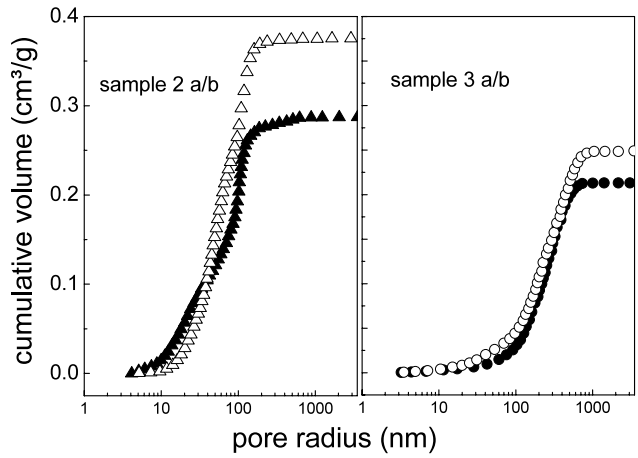

Fig. 5 Cumulative pore volume from Hg-porosimetry. *Filled symbols*: as-prepared samples. *Open symbols*: hydothermally treated

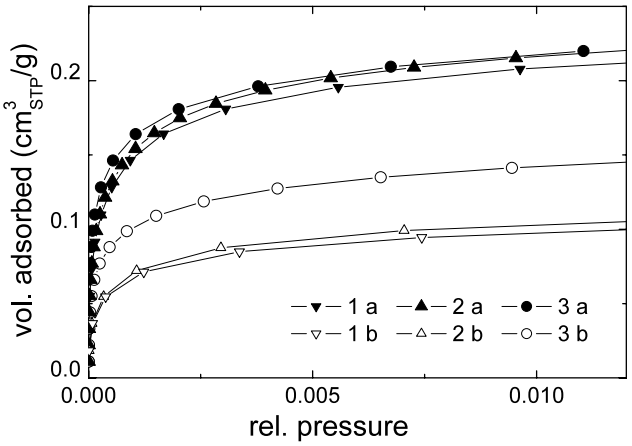

Fig. 6 CO_2 adsorption isotherms at 273 K before and after hydrothermal treatment (equilibration time 120 s)

also the meso- and macropore structure is altered. This effect is well illustrated by results from mercury porosimetry (Table 3), which show that the total pore volume (*including* larger pores) does indeed *increase* during the aging process. Figure 5 also shows differences in the pore size distribution: Within the binder-free material 3, only few cavities are found in the range <100 nm, whereas in the conventional samples 1 (not shown in Fig. 5) and 2 more than 60% of the pore volume accessible to Hg-porosimetry is due to structures of this size. Upon adsorption-desorption cycling, sample 3 exhibits a general increase of pore volume, especially in the range from 10 to 100 nm, whereas sample 2 shows a *decrease* of mesopores <20 nm in combination with a strong *increase* in between 20 and 100 nm, leading to a higher total pore volume.

The finding of major changes to the system of larger pores is also supported by a more detailed study of the kinetics during CO_2 adsorption, revealing an apparent slowing down in adsorption kinetics: While in the case of the as-prepared sample 3a the new equilibrium state at each pressure step is reached within a couple of minutes, the cycled sample 3b still has not attained equilibrium almost an hour after gas dosing. This is well illustrated by Fig. 7, showing the different slopes of the pressure decay curves after gas dosing. Apparently, the structural changes in the course of the aging process lead to an increasing diffusion resistance within the pellet. This was further verified by repeating the experiment on sample material ground to 100–500 μm from the original pellets: Adsorption kinetics remaining almost unchanged, the observed slowing down has to be attributed to hindered diffusion on the meso- or micropore scale. Hence, the CO_2 uptake calculated from automated measurements in the isotherms (Fig. 6) actually strongly depends on the chosen equilibration time. A coarse evaluation of the kinetics indicates two contributions with a largely different diffusion coefficient in case of the cycled sample; in addition, it seems that the total micropore volume of the as-prepared sample (3a) is also detected with CO_2 in the cycled sample (3b) if fully equilibrated.

The results from SAXS measurements (Fig. 8) shed some additional light on the nature of this reordering: the curve in the range of q between 0.1 and 2 nm^{-1}, corresponding to the region of mesopores (i.e. 1.5–30 nm), shows fundamental differences in the aging behaviour between sample 2 and the most stable material 3.

To demonstrate this more clearly, Fig. 8 depicts the scattering intensity multiplied by q^4, yielding a representation where the position of the plateaus as indicated by the dashed lines (Fig. 8) is proportional to the meso- and macropore surface area per volume a_S: While in case of sample 2 only a slight shift of a small hump towards lower q-values (larger length scale) is observed, the binder-free material shows a pronounced surface *increase* in the mesopore region. The position of the additional hump for sample 3b corresponds to

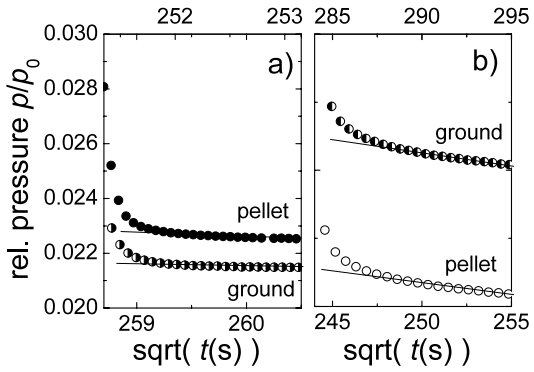

Fig. 7 Pressure decay during CO_2 adsorption for samples 3 a/b. Note the slowing down in case of the hydrothermally treated samples *b*) as well as the similar slopes for ground/pellet samples in either case. The lines indicating the slopes are mere guides to the eye

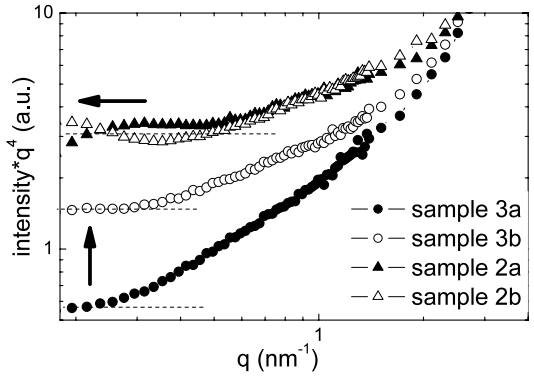

Fig. 8 Comparison of SAXS-data between samples 2 a/b and 3 a/b

a length scale of about 10 nm. Apparently, structural entities of this size are newly formed during hydrothermal cycling.

4 Summary and conclusion

In the present study, we have compared the hydrothermal stability of technical adsorbents of zeolite type 13X from several industrial suppliers under conditions as they arise in heat storage applications. The subsequent characterization has shown that there are significant differences in hydrothermal stability due to the manufacturing process. Material from a so-called binder-free process using LTA-zeolite to obtain mechanical stability has shown best performance in terms of maintaining a high water adsorption capacity. Additional characterization methods such as XRD, CO_2 and N_2 adsorption were also applied, but the agreement with the water adsorption measurements was merely qualitative. However, the results from CO_2 adsorption experiments hint at a dominant kinetic inhibition of the adsorption process as a consequence of repeated hydrothermal stress, to which the measured differences in water uptake may partially be attributed. Apparently, the basic aging process taking place in the open adsorption systems consists the transition of the zeolite component to an X-ray amorphous phase as reported in earlier publications (e.g. Lutz et al. 1988) based on steaming experiments with cristalline samples.

Additionally, the results of this paper shed some light on the role of the binder materials for the rate of hydrothermal destruction: SAXS measurements indicate that in the mesopore region, the structural decomposition process in the binder-free samples differs significantly from the behaviour of conventional adsorbents involving clay minerals as a binder. This is supported by the results from Hg-porosimetry for large mesopores and macropores, which show differences in pore size distribution already in the original state as well as in the evolution of porosity upon hydrothermal cycling.

As no mass transfer out of the adsorbent is possible, this suggests that the X-ray amorphous phase formed during the aging process, which was already reported in previous studies, is of higher density than the original crystalline material, thus creating clefts in the meso- and macropore range in the course of progressing degradation. The much higher amount of macropores (larger than 100 nm) present already in the original state of the binder-free sample represents a major point of distinction to the conventional adsorbents. This is one possible cause for the improved hydrothermal stability: During the desorption step, this larger pore system facilitates diffusion and may thus lead to a similar partial pressure of water vapour within the adsorbent bead as in the surrounding gas stream, whereas in a material showing only narrow access pores, even higher humidity values than imposed by the inlet values will be reached locally inside the adsorbent. Admittedly, this does not account for the observed differences in hydrothermal stability between samples 1 and 2, which appear quite similar by all characterization methods applied in this work. In a follow-up study, the degradation mechanisms will be further investigated e.g. by means of NMR- and IR-spectroscopy. In view of energy storage applications, it is especially required to compare the actual thermal energy storage density before and after hydrothermal treatment via careful determination of adsorption breakthrough curves.

The ensemble of these findings stresses the importance of experiments under close to real application conditions when it gets to the choice of a suitable adsorbent for any thermal energy storage application. The effect of the binder and the manufacturing process on hydrothermal stability proves to be as important as the known influence of ion exchange. Binder-free zeolitic materials appear to be especially promising candidates for this purpose, however, they are very seldomly produced. Improved availability of this kind of adsorbents could contribute remarkably to the further development and more widespread implementation of thermal energy storage in adsorbent materials.

Nomenclature

T_{in}	Air temperature at inlet to test column (°C)
$T_{d,in}$	Dewpoint temperature at air inlet to test column (°C)
x_G	Water content per mass unit of dry air (kg/kg)
x_S	Water uptake per mass unit of dry adsorbent (kg/kg)
$x_{S,des}$	Water content after desorption (kg/kg)
$x_{S,ads}$	Water content after adsorption (kg/kg)
Δh_{ads}	Differential heat of adsorption (kJ/kg)
h_{ads}^{-}	Average heat of adsorption (kJ/kg)
ρ_Q	Energy storage density (kJ/kg)
φ	Relative humidity p/p_0 $(-)$
p	Partial pressure (Pa)
p_0	Saturation pressure at sample temperature (Pa)
θ	Angle of incidence in XRD measurement (°)
a_S	Specific internal surface (m^2/cm^3)
v_S	Specific pore volume (cm^3/g)
q	Scattering vector in SAXS experiment (nm^{-1})

References

Buhl, J.C., et al.: Hydrothermal stability of the novel zeolite type LSX in comparison to the traditional 13X modification. Z. Anorg. Allg. Chem. **630**(4), 604–608 (2004)

Close, D., Dunkle, R.: Adsorbent beds for energy-storage in drying of heating systems. Sol. Energy **19**(3), 233–238 (1977)

Dimitrijevic, R., et al.: Hydrothermal stability of zeolites: Determination of extra-framework species of H–Y faujasite-type steamed zeolite. J. Phys. Chem. Solids **67**(8), 1741–1748 (2006)

Ehrhardt, K., et al.: Hydrothermal decomposition of aluminosilicate zeolites and prediction of their long-term stability. Stud. Surf. Sci. Catal. **94**, 179–186 (1995)

Fichtner-Schmittler, H., et al.: Hydrothermal damage of ion-exchanged a-type zeolite cation-directed mechanisms of phase-transformation. Zeolites **12**(6), 750–755 (1992)

Gartler, G. et al.: Development of a high energy density sorption storage system. In: EuroSun 2004, Freiburg

Haubold, H.-G., et al.: JUSIFA—a new user-dedicated ASAXS beamline for materials science. Rev. Sci. Instrum. **60**, 1943 (1989)

Hauer, A.: Beurteilung fester Adsorbentien in offenen Sorptionssystemen für energetische Anwendungen. Thesis, Technische Universität Berlin (2002a)

Hauer, A.: Thermal energy storage with zeolite for heating and cooling applications. In: R.Z. Wang (ed.) Proc. International Sorption Heat Pump Conference, Shanghai, 2002, pp. 385–390 (2002b)

Jänchen, J., et al.: Studies of water adsorption on zeolites and modified mesoporous materials for seasonal storage of solar heat. Sol. Energy **76**, 339–344 (2004)

Keller, J.U., Staudt, R.: Gas Adsorption Equilibria. Springer, New York (2005), Chap. 1

Lutz, W., et al.: Investigation of the hydrothermal stabilities of NaA, NaCaA and NaMgA zeolites. Chem. Technol. **35**(5), 250–253 (1983)

Lutz, W., et al.: Investigation of hydrothermal stability of synthesized zeolites of type NaCaA. Chem. Technol. **40**(3), 121–125 (1988)

Lutz, W., et al.: Investigation and modeling of the hydrothermal stability of technically relevant zeolites. Adsorption **11**(3–4), 405–413 (2005)

Mugele, J.: Optimierung von Speichermaterialien für den Einsatz in einem thermo-chemischenWärmespeicher für gebäudetechnische Anwendungen. Thesis, Technische Universität Berlin (2004)

Nuñez, T., Henning, H.-M., Mittelbach, W.: High energy density heat storage system—achievements and future work. In: Proc. ISES Solar World Congress 2003, Göteborg

Richtermendau, J., et al.: The pseudomorphous phase-transformation of faujasite-type zeolites in processes of their crystal destruction. Cryst. Res. Technol. **23**(10–11), 1245–1252 (1988)

Stach, H.J. et al.: Influence of cycle temperatures on the thermochemical heat storage densities in the systems water/microporous and water/mesoporous adsorbents. Adsorption **11**(3–4), 393–404 (2005)

Wolf, F., et al.: Über die thermische Stabilität von Molekularsieben des Typs A in Gegenwart von Wasserdampf. Chem. Technol. **2**, 83–87 (1967)